Institutional Repository - Research Portal
Dépôt Institutionnel - Portail de la Recherche
researchportal.unamur.be
University of Namur

RESEARCH OUTPUTS / RÉSULTATS DE RECHERCHE

# Brucella abortus depends on pyruvate phosphate dikinase and malic enzyme but not on Fbp and GlpX fructose-1,6-bisphosphatases for full virulence in laboratory models

Zúñiga-Ripa, Amaia; Barbier, Thibault; Conde-Álvarez, Raquel; Martínez-Gómez, Estrella; Palacios-Chaves, Leyre; Gil-Ramírez, Yolanda; Grilló, María Jesús; Letesson, Jean-Jacques; Iriarte, Maite; Moriyón, Ignacio

*Published in:*
Journal of Bacteriology

*DOI:*
10.1128/JB.01663-14

*Publication date:*
2014

*Document Version*
Early version, also known as pre-print

Link to publication

*Citation for pulished version (HARVARD):*
Zúñiga-Ripa, A, Barbier, T, Conde-Álvarez, R, Martínez-Gómez, E, Palacios-Chaves, L, Gil-Ramírez, Y, Grilló, MJ, Letesson, J-J, Iriarte, M & Moriyón, I 2014, 'Brucella abortus depends on pyruvate phosphate dikinase and malic enzyme but not on Fbp and GlpX fructose-1,6-bisphosphatases for full virulence in laboratory models', *Journal of Bacteriology*. https://doi.org/10.1128/JB.01663-14

**General rights**
Copyright and moral rights for the publications made accessible in the public portal are retained by the authors and/or other copyright owners and it is a condition of accessing publications that users recognise and abide by the legal requirements associated with these rights.

- Users may download and print one copy of any publication from the public portal for the purpose of private study or research.
- You may not further distribute the material or use it for any profit-making activity or commercial gain
- You may freely distribute the URL identifying the publication in the public portal ?

**Take down policy**
If you believe that this document breaches copyright please contact us providing details, and we will remove access to the work immediately and investigate your claim.

Download date: 24. Sep. 2023

JB Accepts, published online ahead of print on 16 June 2014
J. Bacteriol. doi:10.1128/JB.01663-14
Copyright © 2014, American Society for Microbiology. All Rights Reserved.



# *Brucella abortus* depends on pyruvate phosphate dikinase and malic enzyme but not on Fbp and GlpX fructose-1,6-bisphosphatases for full virulence in laboratory models

Amaia Zúñiga-Ripa,[1] Thibault Barbier,[2] Raquel Conde-Álvarez,[1] Estrella Martínez-Gómez,[1] Leyre Palacios-Chaves,[1§] Yolanda Gil-Ramírez,[1¥] María Jesús Grilló,[3] Jean-Jacques Letesson,[2] Maite Iriarte,[1,‡] and Ignacio Moriyón[1,‡,*]

[1] Departamento de Microbiología e Instituto de Salud Tropical, Universidad de Navarra, 31008 Pamplona, Spain.

[2] Research Unit in Biology of Microorganisms – URBM, NARILIS, UNAmur, B-5000 Namur, Belgium.

[3] Grupo de Sanidad Animal, Instituto de Agrobiotecnología (CSIC-Universidad Pública de Navarra-Gobierno de Navarra). Campus de Arrosadía, 31006, Pamplona, Spain.

[§] Present address: Center for Infection and Immunity, Queen's University Belfast Health Sciences Building, 97 Lisburn Rd. Belfast, UK BT9 7AE, UK

[¥] Present address: Lev2050, CEIN, 31110, Noain, Spain.

[‡]These authors contributed equally to this work

[*]**Corresponding author:** Ignacio Moriyón. Mailing address. Departamento de Microbiología y Parasitología, Universidad de Navarra, C/ Irunlarrea 1, 31008 Pamplona, Spain, Phone: +34 948425600 (ext. 806356); Fax: +34 948 425649

Email address: imoriyon@unav.es

Key words: *Brucella*, metabolism, virulence, intracellular, pyruvate phosphate dikinase, malic enzyme, glyoxylate, gluconeogenesis, phosphoenolpyruvate carboxykinase, fructose bisphosphatase.

Running title: *Brucella* metabolism in virulence models

JB Accepts published online ahead of print

JB Accepts published online ahead of print



**ABSTRACT**

The brucellae are the etiological agents of brucellosis, a worldwide-distributed zoonosis. These bacteria are facultative intracellular parasites, and thus are able to adjust their metabolism to the extra and intracellular environments encountered during an infectious cycle. However, this aspect of *Brucella* biology is imperfectly known and the nutrients available in the intracellular niche are unknown. Here, we investigated the central pathways of C metabolism used by *Brucella abortus* by deleting the putative fructose-1,6-bisphosphatases (*fbp* and *glpX*), phosphoenolpyruvate carboxykinase (*pckA*), pyruvate phosphate dikinase (*ppdK*) and malic enzyme (*mae*) genes. In gluconeogenic but not in rich media, growth of mutants Δ*ppdK* and Δ*mae* was severely impaired and growth of the double Δ*fbp*-Δ*glpX* mutant was reduced. In macrophages, only Δ*ppdK* and Δ*mae* showed reduced multiplication, and studies with Δ*ppdK* confirmed that it reached the replicative niche. Similarly, only Δ*ppdK* and Δ*mae* were attenuated in mice, the former being cleared by week 10 and the latter persisting longer than 12 weeks. We also investigated the glyoxylate cycle. Although *aceA* (isocitrate lyase) promoter activity was enhanced in rich medium, *aceA* disruption had no effect *in vitro* or on multiplication in macrophages or mouse spleens. The results suggest that *B. abortus* grows intracellularly using a limited supply of 6 C (and 5 C) sugars that is compensated by glutamate and possibly other amino acids entering the Krebs cycle without a critical role of the glyoxylate shunt.

JB Accepts published online ahead of print



## INTRODUCTION

*Brucella* is a genus of gram-negative bacteria that groups the causative agents of brucellosis, a worldwide-extended zoonosis severely affecting animal production and human welfare. Three species, *B. abortus*, *B. melitensis* and *B. suis*, are the most common causes of brucellosis in domestic livestock and humans. These brucellae can grow both *in vitro* and within host cells, and their pathogenicity results largely from their capacity to escape a prompt detection by innate immunity and the use of a type IV secretion system to reach the replicative niche, an endoplasmic reticulum derived vacuole (1-6). In this compartment, these bacteria multiply extensively, which shows their ability to use efficiently substrates provided by the host. However, there is only sparse information on either the nature of these substrates or the metabolic pathways used in the replicative niche (7).

*In vitro*, most strains of *B. abortus*, *B. melitensis* and *B. suis* grow in several simple chemically defined media (8). Among these, Gerhardt's medium contains glycerol, lactate, glutamate and mineral salts plus nicotinic acid, thiamine, pantothenic acid and biotin as growth factors. This medium supports growth better than other simple defined media, including those that provide glucose as the C source (8), and this has been attributed to the ability of these bacteria to use glutamate very efficiently through the tricarboxylic acid cycle (TCA) (9). Indeed, growth in this medium is clear proof of the ability of these bacteria to carry out gluconeogenesis *in vitro*. Concerning the catabolism of glucose, it has been accepted that it proceeds through the pentose phosphate pathway (in conjunction with TCA), rather than through the glycolysis or Entner–Doudoroff pathways (Fig. 1). This view, although supported by early radiorespirometric and enzymatic studies (10,11) performed with the attenuated *B. abortus* S19 vaccine, is not consistent with the presence of the genes putatively encoding all the enzymes of the Entner-Doudoroff pathway (12). It is possible that the multiple defects in S19 (13) and/or the

JB Accepts published online ahead of print



experimental conditions in those early experiments precluded detection of key enzymes of the Entner-Doudoroff pathway (12).

Concerning intracellular metabolism, some data come from randomly obtained mutants that show attenuation in human or mouse macrophages or in HeLa cells. Genes (putative functions) identified in this manner include, in *B. suis* 1330, a *gguA* homologue (*gluP*, presumably involved in sugar uptake), some erythritol catabolism genes, *gnd* (6-phosphogluconate dehydrogenase, required for using glucose through the pentose phosphate pathway), *rbsk* (ribose kinase), *pyc* (anaplerotic pyruvate carboxylase), *pgi* (phosphoglucose isomerase) and genes related to the biosynthesis of amino acids (14-16); in *B. melitensis* 16M, *dbsA* and *ugpA* (ribose and glycerol-3-phosphate transporters, respectively), *glpD* (glycerol-3-phosphate dehydrogenase) and some erythritol catabolism genes (17,18); and in *B. abortus* 2308, *gluP* (previously shown to encode an active glucose and galactose transporter in this species (19)), *gnd* (6-phosphogluconate dehydrogenase), *gltD* (glutamate synthase) and *gcvB* (glycine dehydrogenase) (20). Also in *B. abortus* 2308, *dxs* (an isoprenoid biosynthesis transketolase) and *mocC* (rhizopine or inositol catabolism) were identified as expressed in macrophages using a fluorescent reporter (21).

Proteomic analyses have also provided clues on the metabolism of brucellae in the host. Forty-eight h after infection of mouse macrophages with *B. suis* 1330, Al Dahouk et al. (22) found an important reduction of proteins putatively involved in energy, protein and nucleic acid metabolism. Some exceptions were ribitol kinase, glyceraldehyde-3-P-dehydrogenase and the isocitrate lyase (AceA) of the glyoxylate cycle. However, other studies in *B. suis* 1330 do not support the use of the glyoxylate cycle within host cells (15). Lamontagne et al. (23) analyzed *B. abortus* 2308 protein expression 3, 20 and 44 h after infection of RAW 264.7 macrophages. They found that multiple proteins associated with sugar uptake, TCA, the pentose phosphate shunt and the subsequent generation of pyruvate were down-regulated 3 h after infection. At 24 h, several proteins involved in sugar metabolism and transport were also reduced. Enzymes

associated with protein and amino acid catabolism were mainly increased early (3 h) but also 24 h after infection, when bacteria were already in vacuoles derived from the endoplasmic reticulum. This was also the case of enzymes involved in glutamate synthesis, suggesting conversion of amino acids into glutamate and α-ketoglutarate. Accordingly, amino acid-based alternatives may be the preferred solution for *B. abortus* to derive precursors for the TCA cycle and ancillary routes during the midpoint time course of infection. At later times, the same authors observed an increase in proteins involved in transport, suggesting that the endoplasmic reticulum is able to supply at least some of the substrates required for bacterial growth. Likewise, the pentose phosphate shunt seemed to partially resume its functions.

Although the information given by these studies is valuable, the central metabolic pathways used by *Brucella* during infection remain unclear. The results are contradictory in some cases, as for the glyoxylate cycle or the metabolic activity in cells. In addition, some studies suggest the availability of sugars in the replicative niche whereas others indicate that amino acids could be the preferred C source *in vivo*, which may require a gluconeogenic metabolism. Indeed, apparently conflicting data may result from the use of different host cell lines, different times of analysis, polarity of mutations and other experimental conditions. Moreover, there might be some variation among *B. suis* 1330, *B. melitensis* 16M and *B. abortus* 2308, as suggested by the known differences in oxidative rates of sugars and amino acids (24). In this work, we attempt to answer some aspects of the central metabolic pathways used by *B. abortus* in the host. For this purpose, we focused our research on genes putatively involved in classical gluconeogenesis, the anabolic pathways bridging TCA and the triose-phosphate pathway, and the glyoxylate cycle. We constructed in-frame mutants in genes coding for key enzymes and tested them in complex and chemically defined media and for multiplication within cultured cells and for persistence in the mouse model (25). Together with some of the previous analyses, our observations suggest a model of *B. abortus* metabolism in which, although TCA supplies

JB Accepts published online ahead of print

JB Accepts published online ahead of print



molecules necessary for biosynthesis and subsequent growth, classical fructose-1,6-bisphosphatases Fbp and GlpX are not necessary and 6 and/or 5 C molecules for polymer biosynthesis are obtained mostly from the intracellular milieu.

## MATERIAL AND METHODS

**Bacterial strains and growth conditions.** The bacterial strains and plasmids used in this study are listed in Table 1S (supplemental material), and their origin and characteristics are described in previous works (26-28). The strains resulting from the genetic manipulations described below were characterized according to standard *Brucella* typing procedures: i.e. colonial morphology after 3 days of incubation at 37ºC, crystal violet-oxalate exclusion, urease, acriflavine agglutination, sensitivity to Tb, Wb, Iz and R/C phages, agglutination with anti-A and anti-M monospecific sera, $CO_2$ and serum dependence, and susceptibility to thionin blue, fuchsin and safranin (24). Bacteria were routinely grown in standard Peptone-Yeast Extract-Glucose broth (Biomerieux) or in this media supplemented with agar (TSA). The following antibiotics were used at the indicated concentrations: kanamycin (Km; 50 µg/mL), nalidixic acid (Nal; 25 µg/mL), chloramphenicol (Cm; 20 µg/mL) and/or gentamicin (Genta; 100 µg/mL or 25 µg/mL) (all from Sigma). When needed, media was supplemented with 5% sucrose (Sigma). All strains were stored at – 80ºC in skim milk (Scharlau). To study the phenotype of the metabolic mutants, Peptone-Yeast Extract-Glucose or the medium of Gerhardt (henceforth Glutamate-Lactate-Glycerol) were used (29). The components (for 1 L) of the latter were: glycerol (30 g), lactic acid (5 g), glutamic acid (1.5 g), thiamine (0.2 mg), nicotinic acid (0.2 mg), pantothenic acid (0.04 mg), biotin (0.0001 mg), $K_2HPO_4$ (10 g), $Na_2S_2O_3 \cdot 5H_2O$ (0.1 g), $MgSO_4$ (10 mg), $MnSO_4$ (0.1 mg), $FeSO_4$ (0.1 mg), NaCl (7.5 g). The pH was adjusted to 6.8-7.

**Growth measurements.** Inocula pre-conditioned to the conditions in the test medium (Peptone-Yeast Extract-Glucose, Glutamate-Lactate-Glycerol, Glycerol-Glutamate, Glycerol-Lactate or Glutamate-Lactate) were prepared as follows. First, the strains to be tested were inoculated into

10 mL of Peptone-Yeast Extract-Glucose in a 50 mL flask and incubated at 37ºC with orbital shaking for 18 h. These exponentially growing bacteria were harvested by centrifugation, resuspended in 5 mL of the test medium at an optical density ($O.D._{600nm}$) of 0.1 and incubated at 37ºC with orbital shaking for 18 h. Then, these pre-conditioned bacteria were harvested by centrifugation, resuspended at an $O.D._{600nm}$ of 0.1 (0.05 starting in the Bioscreen apparatus) in the same test medium in Bioscreen multi-well plates (200 µL/well) and cultivated in a Bioscreen C (Lab Systems) apparatus with continuous shaking at 37ºC. Absorbance values at $420\text{-}580_{nm}$ were automatically recorded at 0.5 h intervals over a 120 to 300 h period. All experiments were performed in triplicate. Controls with culture medium and no bacteria were included in all experiments.

**DNA manipulations**. Genomic sequences were obtained from the Kyoto Encyclopedia of Genes and Genomes (KEGG) database (http://www.genome.jp/kegg/). Searches for DNA and protein homologies were carried out using the National Center for Biotechnology Information (NCBI; http://www.ncbi.nlm.nih.gov/) and the European Molecular Biology Laboratory (EMBL) - European Bioinformatics Institute server (http://www.ebi.ac.uk/). Primers were synthesized by Sigma-Genosys (Haverhill, UK). DNA sequencing was performed by the "Servicio de Secuenciación del Centro de Investigación Médica Aplicada" (Pamplona, Spain). Restriction-modification enzymes were used under the conditions recommended by the manufacturer. Plasmid and chromosomal DNA were extracted with Qiaprep spin Miniprep (Qiagen) and Ultraclean Microbial DNA Isolation kits (Mo Bio Laboratories), respectively. When needed, DNA was purified from agarose gels using the Qiack Gel extraction kit (Qiagen).

In-frame deletion mutants in *fbp* and *glpX* were constructed by polymerase-chain reaction (PCR) overlap using genomic DNA of *B. abortus* 2308 as the DNA template. Primers were designed using the *B. abortus* 2308 sequences available in KEGG (http://www.genome.jp/kegg/). For the construction of the *fbp* mutant, two PCR fragments were

JB Accepts published online ahead of print

JB Accepts published online ahead of print



generated: oligonucleotides *fbp*-F1(5′-GTAGCCAAAAAGCCCAGGT-3′) and *fbp*-R2 (5′-GCCAACCAGAACCAGAGGA-3′) were used to amplify a 203 bp fragment including codons 1–14 of the *fbp* ORF as well as a 161 bp fragment upstream of the *fbp* start codon, and oligonucleotides *fbp*-F3 (5′-TCCTCTGGTTCTGGTTGGCGTGGCCGAAGAGGTGGATA-3′) and *fbp*-R4 (5′-CATTTGCCGCTTCCATGA-3′) were used to amplify a 193 bp fragment including codons 327-341 of the *fbp* ORF and a 148 bp fragment downstream of the *fbp* stop codon. Both fragments were ligated by PCR using oligonucleotides *fbp*-F1 and *fbp*-R4 for amplification, and the complementary regions between *fbp*-R2 and *fbp*-F3 for overlapping. The resulting fragment, containing the *fbp* deletion allele, was cloned into pCR2.1 (Invitrogen) to generate plasmid pAZI-1, sequenced to ensure that the reading frame was maintained, and subcloned into the *Bam*HI and the *Xba*I sites of the suicide plasmid pJQKm (30). The resulting mutator plasmid (pAZI-2) was introduced into *B. abortus* 2308 by conjugation (26). Integration of the suicide vector was selected by Nal and Km resistance, and the excisions (generating both the *fbp* mutant [*BAB*Δ*fbp*] and a sibling revertant strain carrying an intact gene [*BABfbp*-sibling revertant]) were then selected by Nal and sucrose resistance and Km sensitivity. The resulting colonies were screened by PCR with primers *fbp*-F1 and *fbp*-R4, which amplified a fragment of 396 bp in the mutant and a fragment of 1332 bp in the sibling revertant strain. The mutation resulted in the loss of about 98% of the *fbp* ORF and the mutant strain was called *BAB⊿fbp*.

The *glpX* mutant was constructed in a similar way. Primers *glpX*-F1 (5′-ACGGTGATTCTGGTGACACA-3′) and *glpX*-R2 (5′-CGAGCTCCAGTGTGAGAATG-3′) were used to amplify a 576 bp fragment including 61 bp of the *glpX* ORF as well as 515 bp upstream of the *glpX* start codon, and primers *glpX*-F3 (5′-CATTCTCACACTGGAGCTCGATACGACAGATCCGGACGAG-3′) and *glpX*-R4 (5′-CATCATACAGTTGCCGATGG-3′) were used to amplify a 574 bp fragment including 371 bp of the *glpX* ORF and 203 bp downstream of the *glpX* stop codon. Both fragments were ligated by

JB Accepts published online ahead of print



overlapping PCR using primers *glpX*-F1 and *glpX*-R4, and the fragment containing the deletion allele was cloned into pCR2.1 to generate plasmid pAZI-3, sequenced to confirm that the *glpX* ORF had been maintained, and subcloned in pJQKm to produce the mutator plasmid pAZI-4. This plasmid was then introduced into *B. abortus* 2308 and the deletion mutant generated by allelic exchange was selected by Nal and sucrose resistance and Km sensitivity and by PCR using oligonucleotides *glpX*-F1 and *glpX*-R4, which amplified a fragment of 1150 bp in the deletion strain and a fragment of 1705 bp in the *BABglpX*-sibling revertant strain. The mutation resulted in the loss of approximately 56% of the *glpX* ORF, and the mutant was called *BAB⊿glpX.*

To construct the *BAB⊿fbp⊿glpX* double mutant, the mutator plasmid pAZI-4 was introduced into strain *BAB⊿fbp*. After allelic exchange, the double mutant was selected as described above using primers *glpX*-F1 and *glpX*-R4.

*BAB⊿aceA* was constructed using the same strategy. Oligonucleotides *aceA*-F1 (5′-TGACAAGATATCGCCAAAACAC-3′) and *aceA*-R2 (5′-CGAAGGGATGAGGCTGTAAA-3′) amplified a 238 bp fragment, including codons 1-10 of the *aceA* ORF and 208 bp upstream of the *aceA* start codon. Oligonucleotides *aceA*-F3 (5′-TTTACAGCC TCATCCCTTCGGAAACCGCACAGTTCAAGC-3′) and *aceA*-R4 (5′-GGATCAAGAGATCA CCCCAGT-3′) amplified a 278 bp fragment including codons 420-430 of the ORF *aceA* and 245 bp downstream of the *aceA* stop codon. Both fragments were ligated by overlapping PCR using oligonucleotides *aceA*-F1 and *aceA*-R4. The PCR product was cloned into pCR2.1 to generate pAZI-7, sequenced and subcloned into pJQKm to produce the suicide plasmid pAZI-8. *B. abortus* 2308 mutants were selected by PCR using oligonucleotides *aceA*-F1 and *aceA*-R4. PCR products were 1743 bp in *BABaceA*-sibling revertant strain and 738 bp in *BAB⊿aceA*. This mutation eliminated 78% of the *aceA* ORF.

For the construction of the *pckA* mutant, oligonucleotides *pckA*-F1 (5'-TGTTTGCAGTTTTCCACACC-3'), *pckA*-R2 (5'-AATCGAAGCGGCCTTATTGT-3'), *pckA*-F3 (5'-ACAATAAGGCCGCTTCGATTGACGGCTCGCTGAACAAT-3') and *pckA*-R4 (5'-TCTTGCGA TAACAGCCAAAA-3') were used. Primes *pckA*-F1 and *pckA*-R2 amplified a 219 bp fragment, which included codons 1-13 of the *pckA* ORF and 180 bp upstream of the *pckA* start codon. Primers *pckA*-F3 and *pckA*-R4 amplified a 319 bp fragment including the last 37 codons of the *pckA* ORF and 208 bp downstream of the *pckA* stop codon. Both PCR products were ligated by overlapping PCR using *pckA*-F1 and *pckA*-R4, cloned into pCR2.1 to generate plasmid pAZI-5 and subsequently subcloned into the *Bam*HI and the *Xba*I sites of the suicide plasmid pJQKm. The resulting mutator plasmid pAZI-6 was introduced into *B. abortus* 2308, where it was integrated in the chromosome. A second recombination generated the excision of the plasmid. The resulting colonies were screened by PCR (with *pckA*-F1 and *pckA*-R4) amplifying a fragment of 538 bp in the mutant and a fragment of 1864 bp in the sibling revertant strain. The mutant strain was called *BABΔpckA* and lacked the 71.14% of the *pckA* ORF.

*BABΔppdK* was constructed using primers *ppdK*-F1(5´-CTCCCGATTCATTTTTCACG-3´) and *ppdK*-R2 (5′- TGCTCATTTCAGCCAGGTT-3′) to amplify a 288-bp fragment including the first 103 bp of the *ppdK* ORF, as well as 185 bp upstream of the *ppdK* start codon and primers *ppdK*-F3 (5′-AACCTGGCTGAAATGAGCACGGGTCTCGACTATGTGTCC-3′) and *ppdK*-R4 (5′-TCAACGCATCAAAGCAGAAG-3′) to amplify a 220 bp including the last 86 bp of the *ppdK* ORF and 134 bp downstream of the *ppdK* stop codon. Both fragments were ligated by overlapping PCR using primers *ppdK*-F1 and *ppdK*-R4 and the fragment obtained, containing the deletion allele, was cloned into pCR2.1 to generate pMZI-1, sequenced to confirm that the reading frame had been maintained, and subcloned into pJQKm to produce the mutator plasmid pMZI-2. This plasmid was introduced into *B. abortus* 2308 and both the deletion mutant and the sibling revertant strain generated by allelic exchange was selected by Nal and sucrose resistance and

JB Accepts published online ahead of print

Km sensitivity, and by PCR using *ppdK*-F1 and *ppdK*-R4 which amplified a fragment of 508 bp in *BABΔppdK* and a fragment of 2983 bp in *BABppdK*-sibling revertant strain. The mutation generated resulted in the loss of the 93% of *ppdK*.

Primers *ppdKII*-F1 (5'-CTCCCGATTCATTTTTCACG-3'), *ppdKII*-R2 (5'-CTGCTCATTTCAGCCAGGTT-3'), *ppdKII*-F3 (5'-AACCTGGCTGAAATGAGCAGCGGGTCTCGACTATGTGTCC-3') and *ppdKII*-R4 (5'-TCAACGCATCAAAGCAGAAG-3') were used to obtain the mutator plasmid pAZI-10. This plasmid was introduced into *B. abortus* 2308 to obtain a *ppdK* mutant that maintained only the 34 first amino acids of PpdK (*BABΔppdK-II)*. This mutant had the same phenotype as the one previously described. Thus, the mutator plasmid pAZI-10 was also introduced into strain *BABΔpckA* carrying the *pckA* mutation to obtain the double mutant *BABΔpckAΔppdK.*

*BABΔmae* was constructed using primers *mae*-F1 (5′-TATGACGGCGCACTTGTCTA-3′) and *mae*-R2 (5′-TCGGATAGCGATGGAAGAAC -3′) to amplify a 341 bp fragment including 76 bp of the *mae* ORF, as well as 265 bp upstream of the *mae* start codon, and primers *mae*-F3 (5′-GTTCTTCCATCGCTATCCGAGCGAAGCCAATCTTCTGGTA -3′) and *mae*-R4 (5′-CGCCATAAAACGAACCTCAA-3′) to amplify a 376 bp including 227 bp of the *mae* ORF and 149 bp downstream of the *mae* stop codon. Both fragments were ligated by overlapping PCR using primers *mae*-F1 and *mae*-R4 and the fragment obtained, containing the deletion allele, was cloned into pCR2.1 to generate pMZI-3, sequenced to confirm that the *mae* ORF had been maintained, and subloned into pJQKm to produce the mutator plasmid pMZI-4. This plasmid was then introduced into *B. abortus* 2308 and the mutant and sibling revertant strains generated by allelic exchange were selected by Nal and sucrose resistance and Km sensitivity and by PCR using oligonucleotides *mae*-F1 and *mae*-R4, which amplified a fragment of 717 bp in the deleted strain and a fragment of 2739 bp in the sibling revertant strain. The mutation generated resulted in the loss of the 87% of the *mae* ORF.

JB Accepts published online ahead of print

JB Accepts published online ahead of print



To check the different mutations, we used internal primers (*gene*-R5) hybridizing in the deleted regions.

For complementation, a plasmid carrying *ppdK* was constructed using the Gateway cloning Technology (Invitrogen). Since the sequence of *ppdK* from *B. abortus and B. melitensis* is 99% identical, the clone carrying *ppdK* was extracted from the *B. melitensis* ORFEOMA and the ORF subcloned into plasmid pRH001 (31) to produce plasmid pAZI-19. This plasmid was introduced into *BAB*Δ*ppdK* by mating with *E. coli* S17 λ*pir* and the conjugants harboring this plasmid (designated as *BAB*Δ*ppdK* pAZI-19) were selected by plating the mating mixture onto tryptic soy agar (TSA)-Nal-Km plates. For the construction of *BAB*Δ*fbp*Δ*glpX* pAZI-21, gene *fbp* was amplified from *BAB*-parental using primers *fbp*-Fp (5′-GGGATCCATGCTTCTGAAAGGGTGGTACCG-3′) and *fbp*-R4 (5′-CATTTGCCGCTTCCATGA-3′) and cloned into pCR2.1. The resulting plasmid was sequenced, and the *fbp* gene was subcloned into the *Bam*HI and the *Xho*I sites of the vector pBBR1MCS1. The resulting plasmid (pAZI-21) was introduced into *BAB*Δ*fbp*Δ*glpX* by conjugation (see above). *BAB*Δ*fbp*Δ*glpX* pAZI-23 was constructed following the same strategy using primers *glpX*-F1 (5′-ACGGTGATTCTGGTGACACA-3′) and *glpX*-R4 (5′-CATCATACAGTTGCCGATGG-3′) to amplify *glpX*.

**Gene expression studies.** To determine whether *aceA* was expressed *in vitro,* its promoter was fused with the luciferase reporter gene. To this end, *aceA*p-F (5'-GGGATCCTAGTTGCGCTCGATCAGATT-3') and *aceA*p-R (5'-TTCTAGACATTTCGGTGTCTCCTCGT-3') (respectively containing *Bam*HI and *Xba*I sites; underlined) were used to amplify a 382bp region containing the ATG and the *aceA* promoter from *B. abortus* 2308 genomic DNA. This PCR product was verified by electrophoresis and ligated into the vector pGEM-T Easy (Promega), thereby originating plasmid pAZI-17. Then, the insert was digested with *Bam*HI and *Xba*I and ligated to the pSKOriTKmluxAB to generate

plasmid pAZI-18. This plasmid was introduced into *E.coli* S17λ *pir* $Nal^S$ and then transferred by conjugation to *B. abortus* 2308 $Nal^R$ $Km^S$. Cells were plated on TSA NalKm. Positive clones gave a 510 bp band when verified by PCR using *aceA*p-F and *luxAB*-R. The resulting strain was called *B. abortus* p*BABaceA-luxAB.* To measure luciferase activity, fresh *B. abortus* p*BABaceA-luxAB* were adjusted ($OD_{600nm}$) to 0.4 in saline and finally, 50 or 200 µL were added to flasks with 10 mL of Peptone-Yeast Extract-Glucose or Glutamate-Lactate-Glycerol, respectively. Growth was followed by measuring absorbance at $OD_{600nm}$ and 1 mL aliquots were taken at selected intervals to measure the luminescence in Relative Luminescence Units (RLU) after addition of 100 µL ethanol:decanal (1:1).

**Cell infections and intracellular trafficking.** *In vitro* infection assays were performed in RAW 264.7 macrophages (ATCC TIB-71) and HeLa cells (ATCC CCL-2) cultured in Dulbecco's Modified Eagle Medium (DMEM; Gibco) with 10% (v/v) heat-inactivated fetal bovine serum (Gibco), 1% (v/v) L-glutamine 200 nM (Sigma Aldrich) and 1% (v/v) non-essential amino acids (Gibco). Then, 24-well plates were seeded with $1 \times 10^5$ cells/well, and macrophages and HeLa cells were infected at a multiplicity of infection of 50:1 and 200:1 (bacteria:cell), respectively, by centrifuging the plates at $400 \times g$ for 10 min at 4°C. After incubation for 15 min at 37°C under a 5% $CO_2$ atmosphere, extracellular bacteria were removed with four DMEM washes followed by Genta treatment (100 µg/mL) for 90 min. Then, fresh medium supplemented with 25 µg/mL of Genta was added and incubation carried on. Two, 24 and 48 h later, cells were washed three times with 100 mM phosphate buffered saline (pH 7.2), lysed with 0.1% (v/v) Triton X-100 in phosphate buffered saline, and plated on TSA to determine the number of intracellular bacteria. All experiments were performed in triplicate (32). Results were expressed as mean and standard error (n=3) of individual $\log_{10}$ CFU/well. Statistical comparison of means was performed by a one-way ANOVA followed by the Fisher's Protected Least Significant Differences (PLSD) tests (33).

JB Accepts published online ahead of print

JB Accepts published online ahead of print



For immunofluorescence microscopy, RAW 264.7 macrophages and HeLa cells were grown on coverslips and inoculated with bacteria as described above. Cells were fixed in 3% paraformaldehyde in 100 mM phosphate buffered saline (pH 7.2) at 37°C for 10 min. Cells were washed twice with phosphate buffered saline and permeabilized with 0.1% (v/v) Triton X-100 and 3% bovine serum albumin (Sigma), for 30 min. Coverslips were incubated with primary antibodies for 45 min at room temperature, washed three times in the same phosphate buffered saline supplemented with 3% bovine serum albumin, and then incubated with the appropriate secondary antibodies. Coverslips were washed three times with phosphate buffered saline and once with $H_2O$ and mounted onto glass slides using Mowiol 4–88. Samples were examined and images acquired using a Leica TCS SP5 laser scanning confocal microscope at the “UNAmur“ (Namur, Belgium). The primary antibodies used for immunofluorescence microscopy were rabbit anti-calnexin (SPA-860, Stressgen) and a mouse anti-S-LPS monoclonal antibody (A76/12G12/F12). The secondary antibodies were donkey anti-rabbit IgG conjugated to Alexa Fluor 488, (Invitrogen), and goat anti-mouse IgG conjugated to Alexa Fluor 546 (Invitrogen). For lysosomal labeling, the primary antibody used was rat anti-mouse (DBHS) and the secondary antibody was goat anti-rat anti IgG conjugated to Alexa Fluor 633 (Invitrogen).

**Assays in mice.** Female BALB/c mice (Charles River, France) were kept in cages with water and food *ad libitum*, and accommodated under P3 biosafety containment conditions 2 weeks before and during the experiments, in the facilities of the "Instituto de Agrobiotecnología" (registration code ES/31-2016-000002-CR-SU-US). The animal handling and other procedures were in accordance with the current European (directive 86/609/EEC) and Spanish (RD 53/2013) legislations, supervised by the Animal Welfare Committee of the "Universidad Pública de Navarra", and authorized by the competent authority of "Gobierno de Navarra". To prepare inocula, TSA grown bacteria were harvested, adjusted spectrophotometrically ($O.D._{600nm}$ =0.170) in 10 mM phosphate buffered saline (pH 6.85) and diluted in the same diluent up to

JB Accepts published online ahead of print



365 approximately $5 \times 10^5$ colony forming units (CFU)/mL (exact doses were assessed
366 retrospectively).For each bacterial strain, five mice were intraperitoneally inoculated with 0.1
367 mL/mouse and the CFU number in spleen was determined at different weeks post-inoculation as
368 described previously (33). The identity of the spleen isolates was confirmed by PCR. The
369 individual number of CFU/spleen was normalized by logarithmic transformation, and the mean
370 log CFU/spleen values and the standard deviation were calculated for each group of mice (n=5).
371 Statistical comparisons were performed by a one-way ANOVA followed by the Fisher's
372 Protected Least Significant Differences (PLSD) tests (33).

373 **RESULTS**

374 **Dysfunction of *B. abortus fbp*, *glpX*, *ppdK* and *mae* but not of *pckA* or *aceA* homologues**
375 **affects growth on gluconeogenic substrates *in vitro*.** The conversion of fructose-1,6-bisP
376 into fructose-6-P mediated by the cognate bisphosphatase(s) (FBPases) is the only irreversible
377 step among those taking part in gluconeogenesis in *Brucella* (Fig. 1). Therefore, FBPase activity
378 is strictly necessary to grow under gluconeogenic conditions.

379 As in *E. coli* and *Salmonella,* the *B. abortus* 2308 genome presents two ORFs of putative
380 FBPases: BAB2_0364 and BAB1_1292. The former is predicted to encode a protein of 340
381 amino acids that belongs to the class I FBPases (Fbp), and the latter a 328 amino acid protein
382 ortholog to *E. coli* GlpX, a FBPase of class II (Fig. 1). In *E. coli*, Fbp is connected to the
383 production of fructose-6-phosphate for nucleotide, polysaccharide and aromatic amino acid
384 biosynthesis. GlpX, on the other hand, belongs to an operon (*glpFKX*) related to phospholipid
385 biosynthesis (34). The putative *B. abortus glpX*, however, seems isolated and not part of any
386 obvious operon.

387 We constructed mutants carrying in frame deletions in the putative *fbp* (*BABΔfbp* mutant)
388 and *glpX* (*BABΔglpX*) as well as in both genes (*BABΔfbpΔglpX*), and tested their growth in a
389 complex (Peptone-Yeast Extract-Glucose) medium and in the chemically defined medium of

JB Accepts published online ahead of print



Gerhardt (Glutamate-Lactate-Glycerol). In the complex medium, the three mutants grew with generation times and final yields similar to those of *B. abortus* 2308 (*BAB*-parental) (Fig. 2A.1). *BAB*-parental showed reduced growth rates and final yields in Glutamate-Lactate-Glycerol, as expected, and we obtained identical results with either *BABΔfbp* or *BABΔglpX* (Fig. 2A.2). On the other hand, *BABΔfbpΔglpX* produced a markedly lower increase in turbidity in the minimal medium (Fig. 2A.2). Complementation with plasmid pAZI-21 carrying *fbp* or with pAZI-23 carrying *glpX* restored the ability to grow in Glutamate-Lactate-Glycerol to levels close to that of the parental strain (Supplemental Material; Fig. S3). These experiments strongly suggest that *B. abortus* Fbp and GlpX are functional, an interpretation reinforced by their reciprocal complementation (i.e., Fbp complemented *BABΔglpX* and, conversely, GlpX complemented *BABΔfbp*). We then tested combinations of two C sources (Glycerol-Glutamate, Glycerol-Lactate or Glutamate-Lactate). Whereas *BABΔglpX* was not affected, *BABΔfbp* showed retarded growth only in the absence of glycerol (i.e. in Glutamate-Lactate; Fig. 3, upper panels). Since GlpX is the FBPase remaining in *BABΔfbp* and this mutant grew normally when glycerol was present, this result suggests that, as in *E. coli* (34), GlpX is related to glycerol metabolism. Finally, although retarded and diminished, the double *BABΔfbpΔglpX* mutant still showed significant growth (Fig. 3, upper panels).

During these experiments we noticed that *BABΔfbpΔglpX* inoculated broths did not produce a homogeneous growth. This was clearly observed when the double mutant was grown in Glutamate-Lactate-Glycerol in side-arm flasks instead of the automated Bioscreen system. Under these conditions, the bacteria formed macroscopic aggregates (Fig. 4) settling on the bottom of the flasks that indicated a profound surface modification consistent with an altered biosynthesis of envelope molecules. In summary, although Fbp and GlpX deficiency did not abrogate bacterial multiplication, they were required not only for full growth but also for production of normal cells.

JB Accepts published online ahead of print



Next, we investigated the pathways that supply pyruvate or PEP for gluconeogenesis. For this purpose, we carried out a genomic search for homologues of the genes encoding the enzymes connecting the TCA cycle and the triose-phosphate pathway in bacteria (Fig. 1). We identified homologues of *pdh* (pyruvate dehydrogenase), *pyk* (pyruvate kinase), *pckA* (phosphoenolpyruvate carboxykinase), *ppdK* (pyruvate-phosphate dikinase), *pyc* (pyruvate carboxylase), and *mae* (malic enzyme) but not of *pyrcK* (pyruvate carboxykinase), *pps* (phosphoenolpyruvate synthase) or *ppc* (phosphoenolpyruvate carboxylase) (Fig. 1). Since Pyc, Pdh and Pyk catalyze irreversible catabolic steps, we studied the *pckA*, *ppdK* and *mae* homologues.

*B. abortus* 2308 BAB1_2091 is annotated as a pseudogene in some data bases (http://www.genome.jp/kegg/) but not in others (http://biocyc.org.). This ORF encodes a protein of 491 amino acids that bears a 77% similarity with the PckA of the phylogenetically related *Agrobacterium tumefaciens*, a protein of 536 amino acids known to be functional (35). However, *B. abortus* BAB1_2091 is separated by a stop codon from an intergenic region that together with BAB1_2090 encodes the last 45 amino acids present in *A. tumefaciens* PckA. The frame-shift that generates this stop codon is present also in all *B. abortus* strains sequenced so far (http://www.genome.jp/kegg/). Nevertheless, *B. abortus* PckA conserves the IGGTSYAGE-KKS domain (amino acids 190 to 202) specifically required for the carboxykinase activity (36) as well as the phosphate binding site (G--G-GKT; amino acids 236 to 243) and ATP and metal binding sites, so that its functionality is not obviously compromised. In contrast, the putative *B. abortus* 2308 PpdK (encoded by BAB1_0525) represents a complete protein of 887 amino acids with the PEP-binding (amino acids 19 to 376) and the TIM-barrel (amino acids 530 to 883) domains characteristic of PEP-utilizing enzymes.

To test whether these ORFs encoded enzymes are required for growth under gluconeogenic conditions, we constructed the non-polar mutants *BAB⊿pckA* and *BAB⊿ppdK*. Moreover, since

JB Accepts published online ahead of print



both PckA and Ppdk catalyze reactions eventually leading to PEP (Fig. 1), we excluded their reciprocal complementation by constructing the double mutant *BAB⊿pckA⊿ppdK*. We then compared the growth of *BAB*-parental and the mutants in Peptone-Yeast Extract-Glucose and in Glutamate-Lactate-Glycerol. Whereas we did not observe differences in the growth of *BABΔpckA* and *BAB*-parental in these two media, both *BABΔppdK* and *BABΔpckAΔppdK* had a markedly reduced growth in Glutamate-Lactate-Glycerol (Fig. 2B). Complementation with plasmid pAZI-19 carrying *ppdK* restored the phenotype (Supplemental Material; Fig. S1), and the sibling revertant control (see Material and Methods) conserved the wild-type phenotype (not shown). These results strongly suggest that PpdK is functional and that, consistent with the frame shift in *pckA*, PckA does not synthesize PEP from oxaloacetate in *B. abortus*. The possibility that the role of *B. abortus* PckA is not detectable under these *in vitro* conditions seems less likely.

We followed a similar strategy to study the putative *mae*. BAB1_1036 encodes a protein of 774 amino acids annotated as a NADP (or NAD)-dependent enzyme involved in malate metabolism (http://www.genome.jp/kegg/; http://biocyc.org/). The N-terminal domain (amino acids 28-160) and the NADP (or NAD)-binding domain (amino acids 172-409) characteristic of the malic enzyme are conserved in the BAB1_1036 predicted protein. Mutant *BABΔmae* (deleted in the region encoding amino acids 26 to 673) displayed a small reduction in growth in Peptone-Yeast Extract-Glucose and a more marked one in Glutamate-Lactate-Glycerol (Fig. 2C). The impairment was not as accentuated as that of *BABΔppdK* (compare Fig. 2 panels B and C). In these experiments, *mae* mutants with the above-described phenotype were consistently obtained and the control sibling revertants of wild-type phenotype recovered after the last recombination event (see Material and Methods and Supplemental Material; Fig. S2). Taken together, these results support the hypothesis that *B. abortus* Mae supplies pyruvate for PpdK to produce PEP for gluconeogenesis, lactate being a complementary source of pyruvate in

JB Accepts published online ahead of print



Glutamate-Lactate-Glycerol (Fig. 1). We tested this hypothesis further by using media containing only two of the three C substrates of this chemically defined medium. *BAB*Δ*mae* did not grow in Glycerol-Glutamate, showed optimal growth in Glycerol-Lactate, and reduced growth in Glutamate-Lactate (Fig. 3, lower panels). These results are fully consistent with the predicted role of Mae (Fig. 1) and suggest that, although *B. abortus* 2308 can use glycerol, glutamate and lactate, provision of the latter cannot completely replace the Mae pathway. This interpretation is also supported by the fact that whereas PpdK dysfunction in *BABΔppdK* severely impaired growth in Glycerol-Lactate and Glutamate-Lactate, this mutant grew in Glycerol-Glutamate (Fig. 3, lower panels), two substrates able to act as sources of PEP and pyruvate through the triose-P and Mae pathways, respectively (Fig. 1). Indeed, all these results are in agreement with the early studies that led to the formulation of the simple medium of Gerhardt as well as with the nutritional studies that showed the preferential use of glutamate and the complementary role of glycerol and lactate in *B. abortus* (9). Also, the demonstration by Marr et al. (37) of the ability of *B. abortus* to generate pyruvate (and alanine) from glutamate supports an activity of Mae in this bacterium (Fig. 1).

Since the putative Mae was active in *B. abortus* 2308, we investigated whether malate replenishment could occur through the classical glyoxylate pathway (Fig. 1) or the PEP-glyoxylate cycle. The latter cycle combines the operation of *PckA* with the glyoxylate cycle enzymes and operates in *E. coli* under conditions of glucose limitation (38). In these pathways, isocitrate lyase (AceA) cleaves isocitrate to yield glyoxylate and succinate, and a malate synthase (AceB) condenses glyoxylate and acetyl-CoA to produce malate (39-41). The genome of *B. abortus* 2308 carries only one putative *aceA* (ORF BAB1_1631) and one putative *aceB* (ORF BAB1_1663). The predicted AceA is a protein of 429 amino acids with 61% identity and 76% similarity to *E. coli* AceA, and it conserves the amino acids required for the enzymatic activity and the assembly of the tetrameric enzyme (42-47). The predicted AceB has 728 amino

JB Accepts published online ahead of print



490 acids with 59% identity and 74% similarity to *E. coli* malate synthase G, and conserves the
491 catalytic site and the amino acids interacting with acetyl-CoA (48,49). Accordingly, we
492 constructed a non-polar *BABΔaceA* mutant truncated in the 409 central amino acids. This
493 mutant did not show growth differences with *BAB*-parental in Peptone-Yeast Extract-Glucose
494 and Glutamate-Lactate-Glycerol (data not shown), even though these media contain acetogenic
495 substrates (glucose, glycerol, lactate and serine, threonine and alanine) (50). Since the genomic
496 analysis strongly suggests the presence of the glyoxylate cycle, we examined this point further
497 by constructing a luciferase reporter under the control of the AceA promoter. Although growth
498 curves were similar, luciferase activity was considerably higher in Peptone-Yeast Extract-
499 Glucose than in Glutamate-Lactate-Glycerol (Fig. 5), as expected if the glyoxylate cycle
500 becomes active on dependence of the abundance of acetogenic substrates. In such a case, the
501 lack of phenotype in complex media could be explained if the glyoxylate cycle plays only a
502 subsidiary role in this rich medium, and the experiments do not rule out that the possibility that it
503 becomes important under other nutritional conditions.

504 **_B. abortus_ mutants in _ppdK_ and _mae_ but not in _fbp_, _glpX_, _pckA_ or _aceA_ show lower**
505 **multiplication rates in macrophages.** *B. abortus* is characteristically able to multiply
506 intracellularly in professional phagocytes (51). We thus investigated the ability of the above-
507 described mutants to multiply in macrophages using the parental strain and the attenuated *virB*
508 mutant (unable to reach the replicating vacuole) as controls. Figure 6A shows that
509 *BABΔfbpΔglpX* replicated like *BAB*-parental, even though these bacteria differed in growth
510 under gluconeogenic conditions *in vitro* (see above). *BABΔppdK* (Fig. 6B) and *BABΔmae* (Fig.
511 6C) multiplied in macrophages, although at lower overall rates than *BAB*-parental both 24
512 ($p<0,0001$) and 48h ($p<0,0001$) after infection. On the other hand, mutation of *pckA* had no
513 effect either by itself or combined with the *ppdK* deletion (Fig. 6B).

JB Accepts published online ahead of print



These results suggest that, albeit impaired in growth, *BABΔppdK* and *BABΔmae* are still able to reach the replicative intracellular niche. Since Mae and PpdK belong to the same pathway, we selected *BABΔppdK* (the mutant blocked in the upper step of the pathway; Fig. 1) to confirm that the metabolic dysfunction did not prevent these bacteria from reaching the endoplasmic reticulum-derived replicating niche. Figure 7A shows that, in contrast to the *virB* mutant, *BABΔppdK* and the parental bacteria were similar in intracellular distribution.

*B. abortus* can also penetrate and multiply in epithelial cells (51). We found that the behavior of *BABΔppdK* in macrophages was reproduced in HeLa cells (Fig 7A and B). In addition, we found that the CFU of the mutant and *BAB*-parental in HeLa cells did not differ 2 h after infection (not shown), indicating that they were similar with regards to penetration.

***B. abortus* mutants in *ppdK* and *mae* but not in *pckA*, *fbp*, *glpX* or *aceA* are attenuated in mice.** Virulent *B. abortus* is able to establish spleen infections in mice that characteristically develop in four phases: (i), onset phase (spleen colonization; first 48 h); (ii), acute phase (from the third day to weeks 2-4 when bacteria reach maximal numbers); (iii), chronic steady phase (weeks 2-4 to 12), where the bacterial numbers plateau; and (iv), chronic declining phase, during which brucellae are eliminated. The ability to induce a marked splenomegaly is also a characteristic of virulent brucellae. (25). Using this model, we first studied the *BABΔfbpΔglpX* mutant and found that it did not differ from *BAB*-parental in either the CFU/speen profile or the splenomegaly induced (Fig. 8A). Similarly, we did not observe attenuation for *BABΔpckA* (Fig. 8B), which is remarkable because *pckA* expression increases in *B. abortus* mutants in BvrR/BvrS, a master regulator of *B. abortus* virulence (52). Nevertheless, this result is consistent with the genomic features of *pckA* and with the above-described experiments *in vitro* and in macrophages.

*BABΔppdK* failed to reach the chronic steady phase typical of virulent brucellae yielding significantly lower CFU counts after week 2 (Fig. 8B). Clearly indicative of the strong attenuation

539 of *BAB*Δ*ppdK*, we did not recover any bacteria from the spleens of 3 out of the 5 mice examined
540 at post-infection week 12, and this mutant induced less splenomegaly than the virulent bacteria
541 (Fig. 8B). Consistent with the observations that showed no additive effect of the mutations of
542 *ppdK* and *pckA* in macrophages or *in vitro*, the results of *BAB*Δ*pckA*Δ*ppdK* in mice paralleled
543 those of *BAB*Δ*ppdK* (Fig. 8B). *BAB⊿mae* produced a CFU/spleen profile that differed from that of
544 either *BAB*-parental or *BAB*Δ*ppdK*. Although not affected in the first 48 h (onset phase; not
545 shown) this mutant showed a lower multiplication rate during the acute phase (Fig. 8C) that was
546 reminiscent of the lower multiplication rates observed in macrophages. Strikingly, even though
547 CFU/spleen numbers were lower than those of the wild type strains, *BAB⊿mae* produced a
548 chronic steady phase with reduced splenomegaly.

549 Finally, we tested *BAB*Δ*aceA* in mice. In a first experiment, the mutant did not show
550 attenuation at weeks 2, 8 and 12 (not shown). It has been reported that isocitrate lyase is
551 essential for *Salmonella* persistence in mice during chronic infection but dispensable for acute
552 lethal infection (53). Similarly, isocitrate lyase is dispensable in the acute phase of
553 *Mycobacterium tuberculosis* infection in lung macrophages of mice but facilitates persistence
554 during the chronic phase (54). Accordingly, we repeated the mouse infections and determined
555 the number of *BAB*Δ*aceA* CFU in spleens 16 and 24 weeks later. However, we did not find any
556 difference between this mutant and the parental strain (not shown). Therefore, even though we
557 did not rule out the possibility that the glyoxylate cycle plays a role under conditions different
558 from those tested *in vitro*, we concluded that this shunt is not essential for *B. abortus*
559 multiplication and persistence in the laboratory models used. Since the PEP-glyoxylate pathway
560 relies on both AceA and PckA, this conclusion can be extended to this cycle.

561 **DISCUSSION**

562 *B. abortus* lacks the genes necessary for the metabolism of glycogen or poly-beta-
563 hydroxyalkanoates, the two C reserve materials used by prokaryotes (55). Thus, these bacteria

JB Accepts published online ahead of print

JB Accepts published online ahead of print



depend on nutrients provided by the host to multiply intracellularly and, accordingly, they need a supply of (at least) 6 C skeletons or to carry out gluconeogenesis. To investigate these possibilities, we deleted ORFs that could be encoding enzymes of critical steps of gluconeogenesis, or of steps providing the necessary precursors. The genomic characteristics of the ORFs analyzed and the phenotypes observed *in vitro* support the hypothesis that they encode FBPases, a pyruvate phosphate dikinase and a malic enzyme of *B. abortus*. Moreover, the analyses in cells show that the proteins coded for by *ppdK* and *mae* become necessary once the replicative niche is reached, as expected from metabolic mutants.

Since FBPases are essential for gluconeogenesis, the observation that growth in gluconeogenic media was not abolished in the Fbp-GlpX double mutant is intriguing and several hypotheses can be considered to explain these results. The existence of a third FBPase is the first and more obvious possibility. Up to now, five different types of FBPases (I to V) have been described in prokaryotes (56). Whereas FBPases of classes IV and V are restricted to *Archaea* and their close hyperthermophilic *Aquifex* bacterial group, many bacteria have dual combinations of class I (Fbp homologues), class II (GlpX homologues), and class III FBPases (34,56). However, a genomic search for *Bacillus subtilis* YydE homologues (the prototype of class III FBPases (57)) in the *Brucellaceae* only revealed an imperfect match (a hypothetical protein of 218 amino acids with a 32% identity with the 671 amino acids in YydE) in *Ochrobactrum anthropi* and none in *Brucella*. This is in agreement with the fact that no bacterial genome has been described to carry a combination of classes I and III (34). Also, it has been described that some *E. coli* carry two class II FBPases (GlpX and YggF (56)) but genomic analysis of all phosphatases in *B. abortus* fail to identify clear candidates for any phosphatase close to GlpX and Fbp (Supplemental Material; Fig. S4). This genomic evidence and the Fbp-GlpX reciprocal complementation (i.e. the fact that only the double mutant shows phenotype *in vitro* in the absence of glycerol) suggest that these are the main and possibly the only FBPases

JB Accepts published online ahead of print



589 in *B. abortus*. An alternative to the third FBPase hypothesis is the existence of an atypical
590 gluconeogenesis less efficient than the classical one. Hypothetically, a fructose-6-P aldolase
591 could take part in gluconeogenesis. This has been described in *E. coli* K-12 where ORF b0825
592 encodes an enzyme that catalyzes the reversible conversion of fructose-6-P to
593 dihydroxyacetone and glyceraldehyde-3-P (58). This aldolase is different from that operating in
594 the pentose-phosphate cycle and its physiological role is uncertain. However, the only
595 homologous in *B. abortus* (ORF BAB1_1813) is annotated as transaldolase and, in addition to
596 the fact that it should represent the enzyme of the pentose-phosphate cycle, the identity (30%) is
597 below the threshold considered to be significant (59). Obviously, a rigorous analysis of these two
598 hypotheses requires enzymatic analysis of double deficient cells. Finally, the significance of the
599 mucoid aggregates produced by the double FBPase mutant cannot be disregarded since this
600 phenotype suggests that the growth observed does not correspond to a natural condition.

601 Bearing in mind that enzymatic analyses are necessary to reach definite conclusions, our
602 results and those of previous works with *B. abortus* 2308 offer insight into some global models of
603 the metabolism of these bacteria during intracellular life in the host.

604 A first model (gluconeogenic model) can be proposed on the ability of *B. abortus* to grow in
605 the defined medium of Gerhardt and on the proteomic studies in macrophages that suggest that
606 *B. abortus* shifts to an amino acid-based metabolism in which the glutamate pool is increased
607 (23). According to this model, molecules like glycerol, lactate or pyruvate and amino acids
608 channeled to oxaloacetate, keto-glutarate or pyruvate are the main substrates, and molecules of
609 6 and 5 C are derived from the latter. In this regard, it is remarkable that dysfunction of two
610 major FBPases did not bring about any perceptible attenuation either in cells or mice. Although
611 the reduced growth of the *BABΔfbpΔglpx* mutant *in vitro* precludes a clear-cut conclusion, the
612 contrasting *in vivo* and *in vitro* multiplication and the mucoid phenotype of the double mutant in
613 the minimal medium are more consistent with models alternative to the gluconeogenic one.

JB Accepts published online ahead of print



614 Moreover, two lines of evidence indicate that glucose (or closely related hexoses) is available in
615 the host. First, a *B. abortus* 2308 (and *B. suis* 1330) GluP (glucose/galactose transporter)
616 mutant has been identified as attenuated in signature tagged experiments in (15,20,20). Second,
617 it has been reported recently that the multiplication of *B. abortus* in alternatively activated
618 macrophages increases when the intracellular glucose levels are artificially increased (60).
619 Based on these observations, an almost opposite model proposes a main role for 6 C sugars in
620 the replicative niche (and 5 C sugars if we assume that the evidence obtained in *B. melitensis*
621 also applies to *B. abortus*; see Introduction). These sugars would provide trioses-phosphate
622 through the pentose phosphate cycle and serve also as precursors for biosynthesis of envelope
623 polymers. This second model, however, does not account for the attenuation observed for the
624 *ppdK* and *mae* mutants, which strongly suggests that molecules necessary for growth are
625 derived from the TCA *in vivo*.

626 A third model proposes that there is a limited supply of 6 C (and 5 C) sugars that is
627 compensated by glutamate, alanine and other amino acids. Those sugars would be used mostly
628 or exclusively for biosynthesis of envelope polymers and for the pentose-phosphate cycle-
629 dependent biosynthetic reactions. This model is consistent with the results of this and previous
630 works. First, the different phenotype of the *B. abortus BABΔfbpΔglpx* double mutant *in vivo* and
631 *in vitro* is more coherent with the hypothesis that classical gluconeogenesis is not extensively
632 used *in vivo*. In addition, the *B. abortus* 2308 *gluP* mutant identified in signature-tagged
633 mutagenesis studies is not clearly attenuated at two weeks post-infection and manifests its
634 attenuation at times (8 weeks) that correspond to the chronic phase (20). This suggests that the
635 bacteria do not depend totally on hexoses for intracellular biosynthetic processes, and that this
636 dependence is manifested at late times perhaps as the result of changes in the replicative
637 vacuole (see below). Indeed, the infection experiments performed in alternatively activated
638 macrophages suggest that, although available, glucose is a limiting factor for *B. abortus* growth

639 at least during the chronic phase (60). Proteomic studies carried out with *B. abortus* 2308 show
640 that expression of two proteins of the dihydroxyacetone kinase complex (Dha) of the PEP-
641 carbohydrate phosphotransferase system (PTS) is reduced throughout infection in macrophages
642 (23). Although this has been interpreted to mean that reduced PTS expression may be the result
643 of a short supply of sugars within the replicative niche, the *Brucella* PTS lacks the sugar
644 permease unit and is likely to act as a regulatory system coordinating C and N metabolism (61).
645 On the other hand, the signature-tagged mutagenesis and proteomic studies show attenuation
646 of a *gltD* (putatively encoding the small subunit of glutamate synthase) mutant (20) and an
647 increment of enzymes involved in increasing the pool of glutamate (23) that are consistent with
648 the model. Finally, this third model accounts for the attenuation of the *ppdK* and *mae* mutants
649 and could also explain in part the differences between the mutants in these two genes that were
650 observed in mice (Fig. 8). Since according to the model sugars are used mostly to construct
651 envelope polymers and for pentose-phosphate cycle derived precursors, additional molecules
652 for biosynthesis must be derived from TCA. PpdK works to produce PEP, which is used to
653 synthesize phenylalanine, tyrosine and tryptophan, glycerolipids and other PEP-derived
654 molecules. Mae supplies pyruvate for PpdK *in vivo* but TCA would not be the only source of
655 pyruvate. This is suggested by the fact that the *mae* mutant was both delayed in reaching the
656 chronic phase of infection and in lower numbers in the spleen during this phase, which contrasts
657 with the inability of the *ppdK* mutant to generate chronic infections. Interestingly, it has been
658 shown recently that, when provided with multiple carbon sources, *Mycobacterium tuberculosis*
659 differentially catabolizes each carbon source through the glycolytic, pentose phosphate, and/or
660 TCA pathways to distinct metabolic fates, and it has been suggested that this ability reflects an
661 adaptation to pathogenicity (62). Indeed, such ability could also be necessary for *B. abortus* to
662 coordinately use the different substrates proposed for this model.

JB Accepts published online ahead of print

JB Accepts published online ahead of print



Although the last model fits the experimental evidence, it is obvious that it represents only a first approach to the situation in the natural hosts because we cannot assume that the niche is static during a chronic infection or uniform among different types of cells. In the above-mentioned signature-tagged mutagenesis studies, Hong et al. (20) have presented evidence for the hypothesis that different set of genes are required during the onset-acute phases and the chronic steady phase. This study identified three putative metabolic genes (*gluP*, *gldD* [see above] and *gcvP*) required during the chronic phase but not markedly during the acute phase of infection. Indeed, both the need of a functional *ppdK* for the infection to progress during the acute phase and the different phenotype of *mae* add further support to the hypothesis that different genes are required to a different extent during the course of infection. Moreover, at least macrophages and trophoblastic cells have been clearly associated with *B. abortus* infection in cattle (63) and the physiological characteristics of these cells are different. Also, different spleen cells become colonized at different times after intraperitoneal inoculation of mice (64). Clearly, research is necessary to investigate these aspects of the relationship between metabolism and intracellular multiplication in *B. abortus* and in other species of the genus.

**ACKNOWLEDGEMENTS**

We are grateful to Professor E. Van Schaftingen for helpful discussions and suggestions. This research was supported by grants from the "Ministerio de Economía y Competitividad" of Spain (AGL2011-30453-C04-00), "Fundación para la Investigación Médica Aplicada" (FIMA) and, in part, by a grant from the "Fond National de la Recherche Scientifique" (FNRS) (convention FRFC N° 2452110, Belgium) and by the Interuniversity Attraction Poles Programme initiated by the Belgian Science Policy Office. A.Z-R., was supported by a post-doctoral grant from FIMA, T.B. has a PhD grant as ‘‘Aspirant du FNRS’’ and L.P-C. and R.C-A. were funded in part by "Departamento de Educación del Gobierno de Navarra" ("Programa ANABASID").

JB Accepts published online ahead of print



687 **REFERENCES**


688 1. **Barquero-Calvo, E., E. Chaves-Olarte, D. S. Weiss, C. Guzmán-Verri, C. Chacón-Díaz,**
689 **A. Rucavado, I. Moriyón, and E. Moreno**. 2007. *Brucella abortus* uses a stealthy strategy
690 to avoid activation of the innate immune system during the onset of infection. PLoS.One.
691 **2**:e631.

692 2. **Conde-Álvarez, R., V. Arce-Gorvel, M. Iriarte, M. Mancek-Keber, E. Barquero-Calvo, L.**
693 **Palacios-Chaves, C. Chacón-Díaz, E. Chaves-Olarte, A. Martirosyan, von Bargen K.,**
694 **M. J. Grilló, R. Jerala, K. Brandenburg, E. Llobet, J. A. Bengoechea, E. Moreno, I.**
695 **Moriyón, and J. P. Gorvel**. 2012. The lipopolysaccharide core of *Brucella abortus* acts as
696 a shield against innate immunity recognition. PLoS.Pathog. **8**:e1002675.

697 3. **De Bolle, X., J. J. Letesson, and J. P. Gorvel**. 2012. Small GTPases and *Brucella* entry
698 into the endoplasmic reticulum. Biochem.Soc.Trans. **40**:1348-1352.

699 4. **Lacerda, T. L., S. P. Salcedo, and J. P. Gorvel**. 2013. *Brucella* T4SS: the VIP pass inside
700 host cells. Curr.Opin.Microbiol. **16**:45-51.

701 5. **Pizarro-Cerdá, J., S. Méresse, R. G. Parton, G. Van der Goot, A. Sola-Landa, I. López-**
702 **Goñi, E. Moreno, and J. P. Gorvel**. 1998. *Brucella abortus* transits through the
703 autophagic pathway and replicates in the endoplasmic reticulum of nonprofessional
704 phagocytes. Infect.Immun. **66**:5711-5724.

705 6. **Starr, T., T. W. Ng, T. D. Wehrly, L. A. Knodler, and J. Celli**. 2008. *Brucella* intracellular
706 replication requires trafficking through the late endosomal/lysosomal compartment. Traffic.
707 **9**:678-694.

708 7. **Barbier, T., C. Nicolas, and J. J. Letesson**. 2011. *Brucella* adaptation and survival at the
709 crossroad of metabolism and virulence. FEBS Lett. **585**:2929-2934.

710 8. **Moreno, E. and I. Moriyón**. 2006. The Genus *Brucella*, p. 315-456. *In*: M. Dworkin, S.
711 Falcow, E. Rosenberg, K. H. Scheleifer, and E. Stackebrandt (eds.), The Prokaryotes: A
712 Handbook on the Biology of Bacteria., vol. 5. Springer.

713 9. **Gerhardt, P.** 1958. The nutrition of brucellae. Bacteriol.Rev. **22**:81-98.

714 10. **Robertson, D. C. and W. G. McCullough**. 1968. The glucose catabolism of the genus
715 *Brucella*. I. Evaluation of pathways. Arch.Biochem.Biophys. **127**:263-273.

716 11. **Robertson, D. C. and W. G. McCullough**. 1968. The glucose catabolism of the genus
717 *Brucella*. II. Cell-free studies with *B. abortus* (S-19). Arch.Biochem.Biophys. **127**:445-456.

718 12. **Essenberg, R. C., R. Seshadri, K. Nelson, and I. Paulsen**. 2002. Sugar metabolism by
719 *Brucellae*. Vet.Microbiol. **90**:249-261.

720 13. **Crasta, O. R., O. Folkerts, Z. Fei, S. P. Mane, C. Evans, S. Martino-Catt, B. Bricker, G.**
721 **Yu, L. Du, and B. W. Sobral**. 2008. Genome sequence of *Brucella abortus* vaccine strain
722 S19 compared to virulent strains yields candidate virulence genes. PLoS.One. **3**:e2193.

14. **Köhler, S., S. Ouahrani-Bettache, M. Layssac, J. Teyssier, and J. P. Liautard**. 1999. Constitutive and inducible expression of green fluorescent protein in *Brucella suis*. Infect.Immun. **67**:6695-6697.

15. **Köhler, S., V. Foulongne, S. Ouahrani-Bettache, G. Bourg, J. Teyssier, M. Ramuz, and J. P. Liautard**. 2002. The analysis of the intramacrophagic virulome of *Brucella suis* deciphers the environment encountered by the pathogen inside the macrophage host cell. Proc.Natl.Acad.Sci.U.S.A **99**:15711-15716.

16. **Foulongne, V., G. Bourg, C. Cazevieille, S. Michaux-Charachon, and D. O'Callaghan**. 2000. Identification of *Brucella suis* genes affecting intracellular survival in an in vitro human macrophage infection model by signature-tagged transposon mutagenesis. Infect.Immun. **68**:1297-1303.

17. **Lestrate, P., R. M. Delrue, I. Danese, C. Didembourg, B. Taminiau, P. Mertens, X. De Bolle, A. Tibor, C. M. Tang, and J. J. Letesson**. 2000. Identification and characterization of *in vivo* attenuated mutants of *Brucella melitensis*. Mol.Microbiol. **38**:543-551.

18. **Wu, Q., J. Pei, C. Turse, and T. A. Ficht**. 2006. Mariner mutagenesis of *Brucella melitensis* reveals genes with previously uncharacterized roles in virulence and survival. BMC.Microbiol. **6**:102.

19. **Essenberg, R. C., C. Candler, and S. K. Nida**. 1997. *Brucella abortus* strain 2308 putative glucose and galactose transporter gene: cloning and characterization. Microbiology **143**:1549-1555.

20. **Hong, P. C., R. M. Tsolis, and T. A. Ficht**. 2000. Identification of genes required for chronic persistence of *Brucella abortus* in mice. Infect.Immun. **68**:4102-4107.

21. **Eskra, L., A. Canavessi, M. Carey, and G. Splitter**. 2001. *Brucella abortus* genes identified following constitutive growth and macrophage infection. Infect.Immun. **69**:7736-7742.

22. **Al Dahouk, S., V. Jubier-Maurin, H. C. Scholz, H. Tomaso, W. Karges, H. Neubauer, and S. Köhler**. 2008. Quantitative analysis of the intramacrophagic *Brucella suis* proteome reveals metabolic adaptation to late stage of cellular infection. Proteomics. **8**:3862-3870.

23. **Lamontagne, J., A. Forest, E. Marazzo, F. Denis, H. Butler, J. F. Michaud, L. Boucher, I. Pedro, A. Villeneuve, D. Sitnikov, K. Trudel, N. Nassif, D. Boudjelti, F. Tomaki, E. Chaves-Olarte, C. Guzmán-Verri, S. Brunet, A. Cote-Martin, J. Hunter, E. Moreno, and E. Paramithiotis**. 2009. Intracellular adaptation of *Brucella abortus*. J.Proteome.Res. **8**:1594-1609.

24. **Alton, G. G., L. M. Jones, R. D. Angus, and J. M. Verger**. 1988. *Techniques for the Brucellosis Laboratory*. Paris:INRA.

25. **Grilló, M. J., J. M. Blasco, J. P. Gorvel, I. Moriyón, and E. Moreno**. 2012. What have we learned from brucellosis in the mouse model? Vet.Res **43**:29.

26. **Conde-Álvarez, R., M. J. Grilló, S. P. Salcedo, M. J. de Miguel, E. Fugier, J. P. Gorvel, I. Moriyón, and M. Iriarte**. 2006. Synthesis of phosphatidylcholine, a typical eukaryotic

JB Accepts published online ahead of print

phospholipid, is necessary for full virulence of the intracellular bacterial parasite *Brucella abortus*. Cell Microbiol. **8**:1322-1335.

27. **Monreal, D., M. J. Grilló, D. González, C. M. Marín, M. J. de Miguel, I. López-Goñi, J. M. Blasco, A. Cloeckaert, and I. Moriyón**. 2003. Characterization of *Brucella abortus* O-polysaccharide and core lipopolysaccharide mutants and demonstration that a complete core is required for rough vaccines to be efficient against *Brucella abortus* and *Brucella ovis* in the mouse model. Infect.Immun. **71**:3261-3271.

28. **Palacios-Chaves, L., R. Conde-Álvarez, Y. Gil-Ramírez, A. Zúñiga-Ripa, E. Barquero-Calvo, C. Chacón-Díaz, E. Chaves-Olarte, V. rce-Gorvel, J. P. Gorvel, E. Moreno, M. J. de Miguel, M. J. Grilló, I. Moriyón, and M. Iriarte**. 2011. *Brucella abortus* ornithine lipids are dispensable outer membrane components devoid of a marked pathogen-associated molecular pattern. PLoS.One. **6**:e16030.

29. **Gerhardt, P. and J. B. Wilson**. 1948. The nutrition of brucellae; growth in simple chemically defined media. J.Bacteriol. **56**:17-24.

30. **Scupham, A. J. and E. W. Triplett**. 1997. Isolation and characterization of the UDP-glucose 4'-epimerase-encoding gene, *galE*, from *Brucella abortus* 2308. Gene **202**:53-59.

31. **Hallez, R., J. J. Letesson, J. Vandenhaute, and X. De Bolle**. 2007. Gateway-based destination vectors for functional analyses of bacterial ORFeomes: application to the Min system in *Brucella abortus*. Appl.Environ.Microbiol. **73**:1375-1379.

32. **Sieira, R., D. J. Comerci, D. O. Sanchez, and R. A. Ugalde**. 2000. A homologue of an operon required for DNA transfer in *Agrobacterium* is required in *Brucella abortus* for virulence and intracellular multiplication. J.Bacteriol. **182**:4849-4855.

33. **Grilló, M. J., L. Manterola, M. J. de Miguel, P. M. Muñoz, J. M. Blasco, I. Moriyón, and I. López-Goñi**. 2006. Increases of efficacy as vaccine against *Brucella abortus* infection in mice by simultaneous inoculation with avirulent smooth *bvrS/bvrR* and rough *wbkA* mutants. Vaccine **24**:2910-2916.

34. **Donahue, J. L., J. L. Bownas, W. G. Niehaus, and T. J. Larson**. 2000. Purification and characterization of *glpX*-encoded fructose 1, 6-bisphosphatase, a new enzyme of the glycerol 3-phosphate regulon of *Escherichia coli*. J.Bacteriol. **182**:5624-5627.

35. **Liu, P., D. Wood, and E. W. Nester**. 2005. Phosphoenolpyruvate carboxykinase is an acid-induced, chromosomally encoded virulence factor in *Agrobacterium tumefaciens*. J.Bacteriol. **187**:6039-6045.

36. **Osteras, M., B. T. Driscoll, and T. M. Finan**. 1995. Molecular and expression analysis of the *Rhizobium meliloti* phosphoenolpyruvate carboxykinase (*pckA*) gene. J.Bacteriol. **177**:1452-1460.

37. **Marr, A. G., C. B. Olsen, H. S. Unger, and J. B. Wilson**. 1953. The oxidation of glutamic acid by *Brucella abortus*. J.Bacteriol. **66**:606-610.

38. **Fischer, E. and U. Sauer**. 2003. A novel metabolic cycle catalyzes glucose oxidation and anaplerosis in hungry *Escherichia coli*. J.Biol.Chem. **278**:46446-46451.

JB Accepts published online ahead of print

39. **Ajl, S. L., J. Rust, Jr., and R. W. Wheat**. 1956. Distribution of the tricarboxylic acid cycle enzymes in extracts of *Escherichia coli*. J.Cell Physiol **47**:317-339.

40. **Smith, R. A. and I. C. Gunsalus**. 1954. Isocitratase: a nex tricarboxylic acid cleavage system. J.Amer.Chem.Soc. **76**:5002.

41. **Kornberg, H. L. and H. A. Krebs**. 1957. Synthesis of cell constituents from C2-units by a modified tricarboxylic acid cycle. Nature **179**:988-991.

42. **Diehl, P. and B. A. McFadden**. 1993. Site-directed mutagenesis of lysine 193 in *Escherichia coli* isocitrate lyase by use of unique restriction enzyme site elimination. J.Bacteriol. **175**:2263-2270.

43. **Diehl, P. and B. A. McFadden**. 1994. The importance of four histidine residues in isocitrate lyase from *Escherichia coli*. J.Bacteriol. **176**:927-931.

44. **Rehman, A. and B. A. McFadden**. 1996. The consequences of replacing histidine 356 in isocitrate lyase from *Escherichia coli*. Arch.Biochem.Biophys. **336**:309-315.

45. **Rehman, A. and B. A. McFadden**. 1997. Serine319 and 321 are functional in isocitrate lyase from *Escherichia coli*. Curr.Microbiol. **34**:205-211.

46. **Rehman, A. and B. A. McFadden**. 1997. Lysine 194 is functional in isocitrate lyase from *Escherichia coli*. Curr.Microbiol. **35**:14-17.

47. **Rehman, A. and B. A. McFadden**. 1997. Cysteine 195 has a critical functional role in catalysis by isocitrate lyase from *Escherichia coli*. Curr.Microbiol. **35**:267-269.

48. **Howard, B. R., J. A. Endrizzi, and S. J. Remington**. 2000. Crystal structure of *Escherichia coli* malate synthase G complexed with magnesium and glyoxylate at 2.0 A resolution: mechanistic implications. Biochemistry **39**:3156-3168.

49. **Tugarinov, V. and L. E. Kay**. 2005. Quantitative $^{13}C$ and $^{2}H$ NMR relaxation studies of the 723-residue enzyme malate synthase G reveal a dynamic binding interface. Biochemistry **44**:15970-15977.

50. **Wolfe, A. J.** 2005. The acetate switch. Microbiol.Mol.Biol.Rev. **69**:12-50.

51. **Moreno, E. and J. P. Gorvel**. 2004. Invasion, intracellular trafficking and replication of *Brucella* organisms in professional and non-professional phagocytes., p. 287. *In*: I. López-Goñi and I. Moriyón (eds.), *Brucella*: Molecular and Cellular Biology. Horizon Bioscience, Wymondham, UK.

52. **Viadas, C., M. C. Rodriguez, F. J. Sangari, J. P. Gorvel, J. M. García-Lobo, and I. López-Goñi**. 2010. Transcriptome analysis of the *Brucella abortus* BvrR/BvrS two-component regulatory system. PLoS.One. **5**:e10216.

53. **Fang, F. C., S. J. Libby, M. E. Castor, and A. M. Fung**. 2005. Isocitrate lyase (AceA) is required for *Salmonella* persistence but not for acute lethal infection in mice. Infect.Immun. **73**:2547-2549.


JB Accepts published online ahead of print

JB Accepts published online ahead of print




838 54. **McKinney, J. D., B. K. Honer zu, E. J. Muñoz-Elías, A. Miczak, B. Chen, W. T. Chan, D.**
839 **Swenson, J. C. Sacchettini, W. R. Jacobs, Jr., and D. G. Russell**. 2000. Persistence of
840 *Mycobacterium tuberculosis* in macrophages and mice requires the glyoxylate shunt
841 enzyme isocitrate lyase. Nature **406**:735-738.

842 55. **Chain, P. S., D. J. Comerci, M. E. Tolmasky, F. W. Larimer, S. A. Malfatti, L. M.**
843 **Vergez, F. Aguero, M. L. Land, R. A. Ugalde, and E. Garcia**. 2005. Whole-genome
844 analyses of speciation events in pathogenic *Brucellae*. Infect.Immun. **73**:8353-8361.

845 56. **Brown, G., A. Singer, V. V. Lunin, M. Proudfoot, T. Skarina, R. Flick, S. Kochinyan, R.**
846 **Sanishvili, A. Joachimiak, A. M. Edwards, A. Savchenko, and A. F. Yakunin**. 2009.
847 Structural and biochemical characterization of the type II fructose-1,6-bisphosphatase
848 GlpX from *Escherichia coli*. J.Biol.Chem. **284**:3784-3792.

849 57. **Fujita, Y., K. Yoshida, Y. Miwa, N. Yanai, E. Nagakawa, and Y. Kasahara**. 1998.
850 Identification and expression of the *Bacillus subtilis* fructose-1, 6-bisphosphatase gene
851 (*fbp*). J.Bacteriol. **180**:4309-4313.

852 58. **Schurmann, M. and G. A. Sprenger**. 2001. Fructose-6-phosphate aldolase is a novel
853 class I aldolase from *Escherichia coli* and is related to a novel group of bacterial
854 transaldolases. J.Biol.Chem. **276**:11055-11061.

855 59. **Rost, B.** 1999. Twilight zone of protein sequence alignments. Protein Eng **12**:85-94.

856 60. **Xavier, M. N., M. G. Winter, A. M. Spees, A. B. den Hartigh, K. Nguyen, C. M. Roux, T.**
857 **M. Silva, V. L. Atluri, T. Kerrinnes, A. M. Keestra, D. M. Monack, P. A. Luciw, R. A.**
858 **Eigenheer, A. J. Bäumler, R. L. Santos, and R. M. Tsolis**. 2013. PPARγ-mediated
859 increase in glucose availability sustains chronic *Brucella abortus* infection in alternatively
860 activated macrophages. Cell Host.Microbe **14**:159-170.

861 61. **Dozot, M., S. Poncet, C. Nicolas, R. Copin, H. Bouraoui, A. Maze, J. Deutscher, X. De**
862 **Bolle, and J. J. Letesson**. 2010. Functional characterization of the incomplete
863 phosphotransferase system (PTS) of the intracellular pathogen *Brucella melitensis*.
864 PLoS.One. **5**.

865 62. **De Carvalho, L. P., S. M. Fischer, J. Marrero, C. Nathan, S. Ehrt, and K. Y. Rhee**. 2010.
866 Metabolomics of *Mycobacterium tuberculosis* reveals compartmentalized co-catabolism of
867 carbon substrates. Chem.Biol. **17**:1122-1131.

868 63. **Enright, F. M.** 1990. The pathogenesis and pathobiology of *Brucella* infection in domestic
869 animals, *In*: K. D. J. Nielsen (ed.), Animal Brucellosis. CRC Press, Boca Raton.

870 64. **Copin, R., M. A. Vitry, Hanot Mambres D., A. Machelart, DeTrez C., J. M.**
871 **Vanderwinden, S. Magez, S. Akira, B. Ryffel, Y. Carlier, J. J. Letesson, and E.**
872 **Muraille**. 2012. *In situ* microscopy analysis reveals local innate immune response
873 developed around *Brucella* infected cells in resistant and susceptible mice. PLoS.Pathog.
874 **8**:e1002575.

875 **FIGURE LEGENDS**

876 **FIG. 1.** Conventional central metabolic pathways (glycolysis, gluconeogenesis, Entner-
877 Doudoroff, pentose-phosphate, TCA and glyxoylate) of bacteria. Dashed arrows indicate steps
878 for which no putative genes can be identified in *B. abortus*. Red arrows indicate the steps
879 studied in this work. Abbreviations used in the figure are: AcCoA (acetyl-CoA), AceA (isocitrate
880 lyase), AceB (malate synthase), Acn (aconitate hidratase), AKG (α-ketoglutarate), Akgdh (α-
881 ketoglutarate dehydrogenase), Cgs (cyclic-glucan synthesis), CIT (citrate), DHAP
882 (dihydroxyacetone phosphate), Eda (keto-deoxy-phosphogluconate aldolase), Edd (6-phospho-
883 D-gluconate dehydratase), E4P (erythrose-4-phosphate), Fba (fructose bisphosphate aldolase),
884 Fbp (fructose-1,6-bisphosphatase), Fum (fumarase), FUM (fumarate), F1,6dP (fructose-1,6-
885 bisphosphate), F6P (fructose-6-phosphate), GalE (UPD-glucose-4 epimerase), GAP
886 (glyceraldehyde-3-phosphate), Gnd (6-phosphogluconate dehydrogenase), Glk (glucokinase),
887 GlpX (fructose-1,6-bisphosphatase), GltA (citrate synthase), GLX (glyoxylate), G1P (glucose-1-
888 phosphate), G6P (glucose-6-phosphate), ICIT (isocitrate), Idh (isocitrate dehydrogenase), KDPG
889 (2-keto-3-deoxyphosphogluconate), LPS (lipopolysaccharide), Mae (malic enzyme), MAL
890 (malate), Mdh (malate dehydrogenase), OAA (oxaloacetate), Pfk (phosphofructokinase), PckA
891 (phosphoenol pyruvate carboxikinase), Pdh ( pyruvate dehydrogenase), PEP (phosphoenol
892 pyruvate), Pgi (phosphoglucose isomerase), Pgl (lactonase), Pgm (phosphoglucomutase), Ppc
893 (phosphoenol pyruvate carboxylase), PpdK (pyruvate phosphate dikinase), Pps (phosphoenol
894 pyruvate synthase), Pyc (pyruvate carboxylase), Pyk (pyruvate kinase), PYR (pyruvate), Pyrck
895 (pyruvate carboxikinase), RIB5P (ribulose-5-phosphate), Sdh (succinate dehydrogenase), Stk
896 (succinyl-CoA synthethase), SUC (succinate), SucCoA (succinyl-CoA), Tkt (transketolase), TpiA
897 (triose phosphate isomerase), X5P (xylulose-5-phosphate), Zwf (glucose-6-phosphate
898 dehydrogenase), 6PG (6-phosphogluconate), 6PGL (6-phosphogluconolactone).
899

JB Accepts published online ahead of print

**FIG. 2.** Growth curves in Peptone-Yeast Extract-Glucose (A.1, B.1 and C.1) and Glutamate-Lactate-Glycerol (A.2, B.2 and C.2) of *BAB*-parental and mutants *BAB*Δ*fbp*, *BAB*Δ*glpX*, *BAB*Δ*fbp*Δ*glpX, BAB*Δ*pckA*, *BAB*Δ*ppdK*, *BAB*Δ*pckA*Δ*ppdK* and *BAB*Δ*mae*. Each point represents the mean ± standard error (error bars are within the size of the symbols) of optical density (O.D.) values of triplicate samples. The experiment was repeated three times with similar results.

**FIG. 3.** Growth curves in Glycerol-Glutamate, Glycerol-Lactate and Glutamate-Lactate of *BAB*-parental and mutants *BAB*Δ*fbp*, *BAB*Δ*glpX, BAB*Δ*fbp*Δ*glpX*, *BAB*Δ*ppdK* and *BAB*Δ*mae*. Each point represents the mean of triplicate samples (error bars are within the size of the symbols). The experiment was repeated three times with similar results.

**FIG. 4.** Immunofluorescence analysis of *BAB*-parental and *BABΔfbpΔglpX* grown in Glycerol-Lactate-Glutamate. Cells were labeled with anti-smooth-lipopolysaccharide mouse monoclonal antibody A76/12G12/F12 and Alexa Fluor 546 conjugated goat anti-mouse immunoglobulin.

**FIG. 5.** Luciferase expression under the control of *B. abortus aceA* promoter in Peptone-Yeast Extract-Glucose and Glutamate-Lactate-Glycerol. The results are representative of three experiments (RLU, relative luminescence units).

**FIG. 6.** Intracellular multiplication in RAW 264.7 macrophages of *BAB*-parental and mutants *BAB*Δ*fbp*Δ*glpX, BAB*Δ*pckA*, *BAB*Δ*ppdK, BAB*Δ*pckA*Δ*ppdK* and BAB*Δmae* (*virB* is an attenuated mutant used as a control). Values are the mean ± standard error of triplicate infections and the results shown are representative of three independent experiments.

JB Accepts published online ahead of print

925 **FIG. 7.** Trafficking of *BAB*-parental, *BAB*Δ*ppdK* and *virB* in macrophages and HeLa cells. (A),
926 confocal images of infected RAW 264.7 macrophages and HeLa cells labeled with Moabs to
927 either calnexin (in green) or LAMP-1 (in blue) 24 hours after infection (bacteria are
928 immunostained in red). (B), Percentage of calnexin-positive vacuoles of HeLa cells that contain
929 bacteria at 24 and 48 hours post-infection.
930
931 **FIG. 8.** Bacterial multiplication (upper panels) and spleen weights (lower panels) generated in
932 BALB/c mice by *BAB*-parental and mutants *BAB*Δ*fbp*Δ*glpX* (A); *BAB*Δ*pckA*, *BAB*Δ*ppdK* and
933 *BAB*Δ*pckA*Δ*ppdK* (B); and *BAB*Δ*mae* (C). Each point is the mean ± standard deviation (n=5) of
934 the Log of CFU or grams per spleen. Statistical differences with *BAB*-parental were significant ($p < 0.001$)
935 from week 4 onwards for *BAB*Δ*ppdK* and from week 2 onwards for *BAB*Δ*mae*.
936 *BAB*Δ*pckA*Δ*ppdK* was also attenuated at weeks 8 and 12 ($p < 0.001$) (weeks 4 and 6 were not
937 tested).

JB Accepts published online ahead of print

JB Accepts published online ahead of print

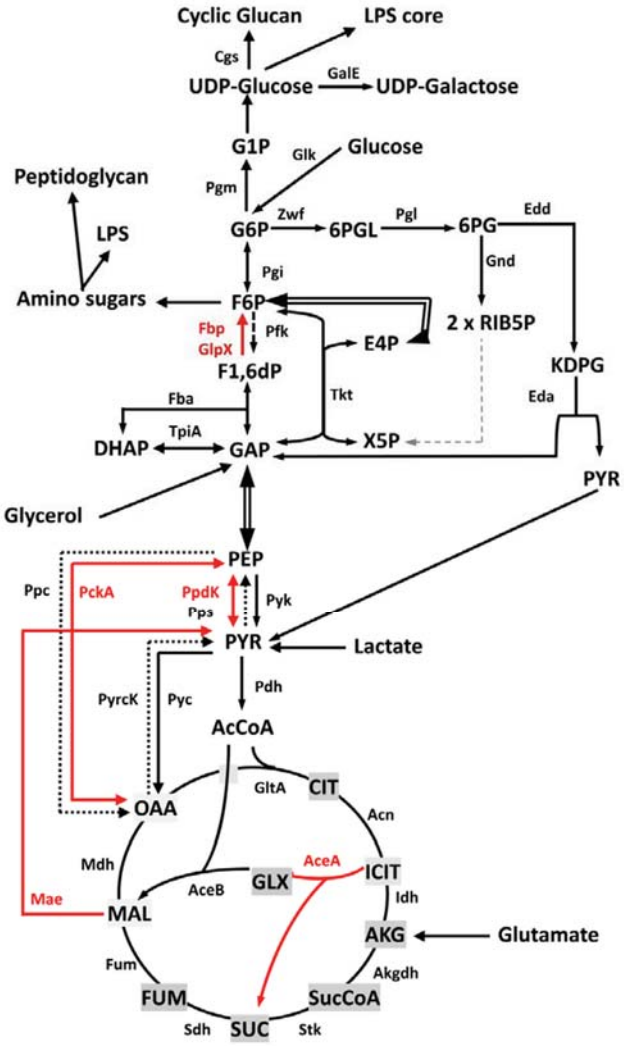

JB Accepts published online ahead of print

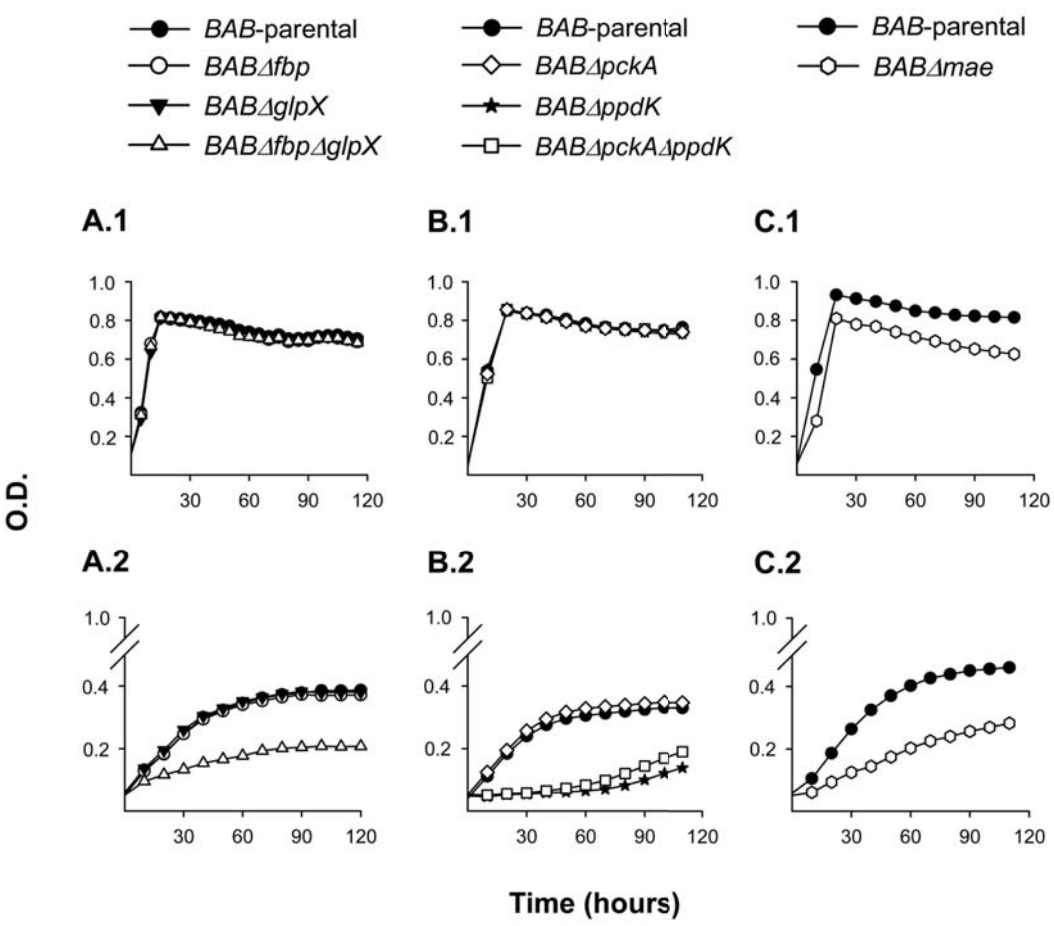

JB Accepts published online ahead of print

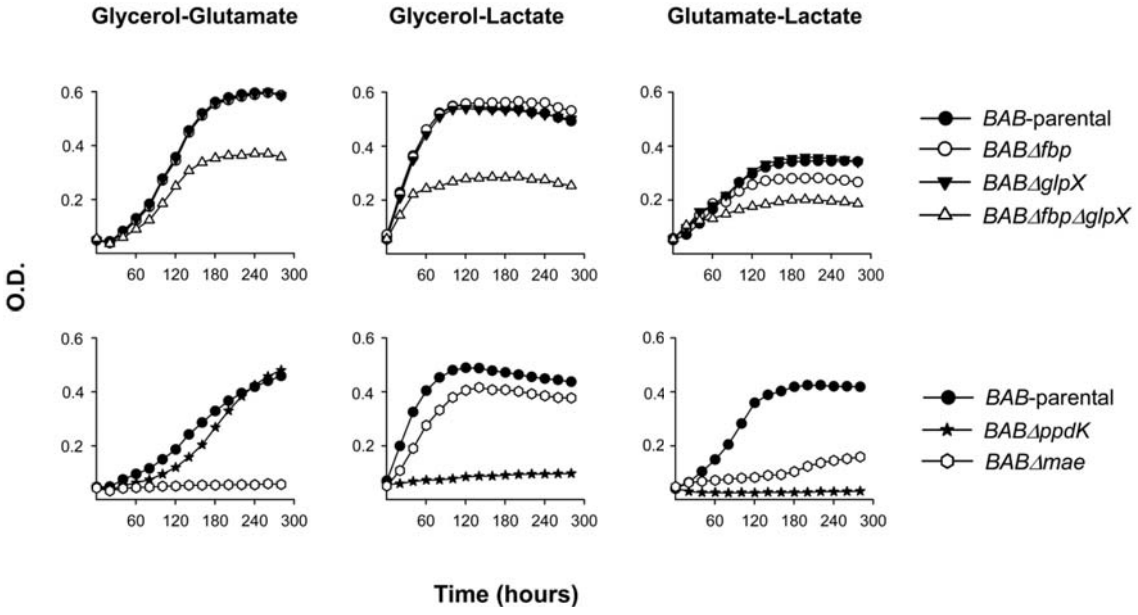

JB Accepts published online ahead of print

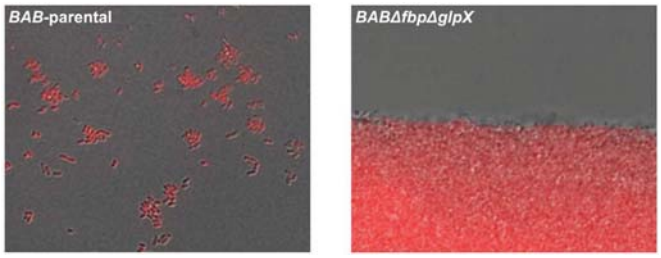

JB Accepts published online ahead of print

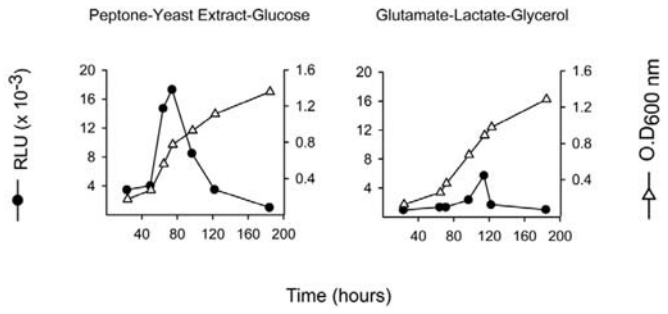

JB Accepts published online ahead of print

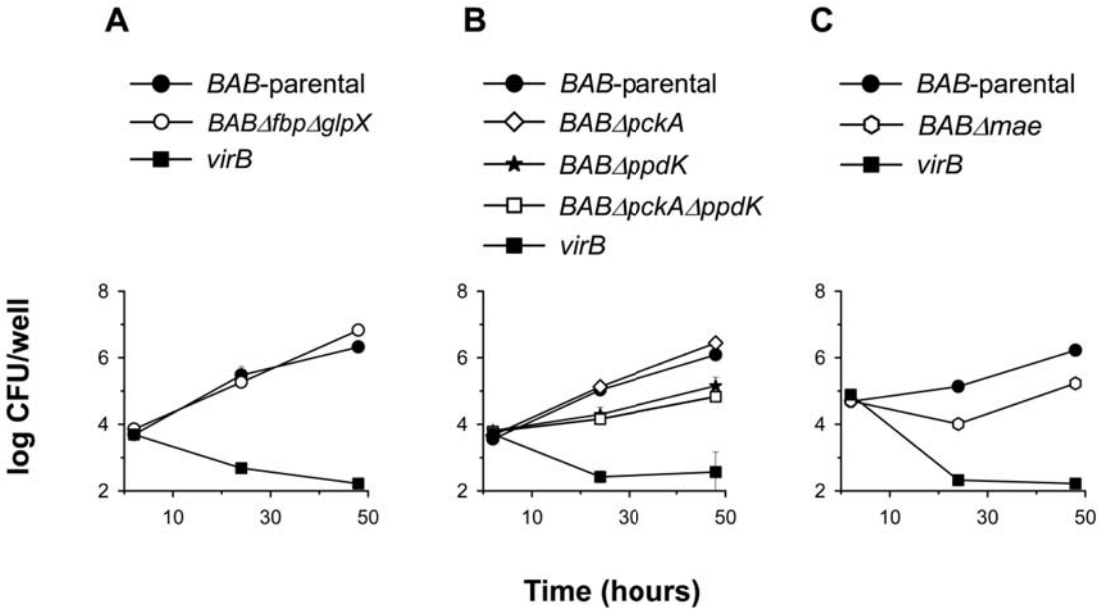

JB Accepts published online ahead of print

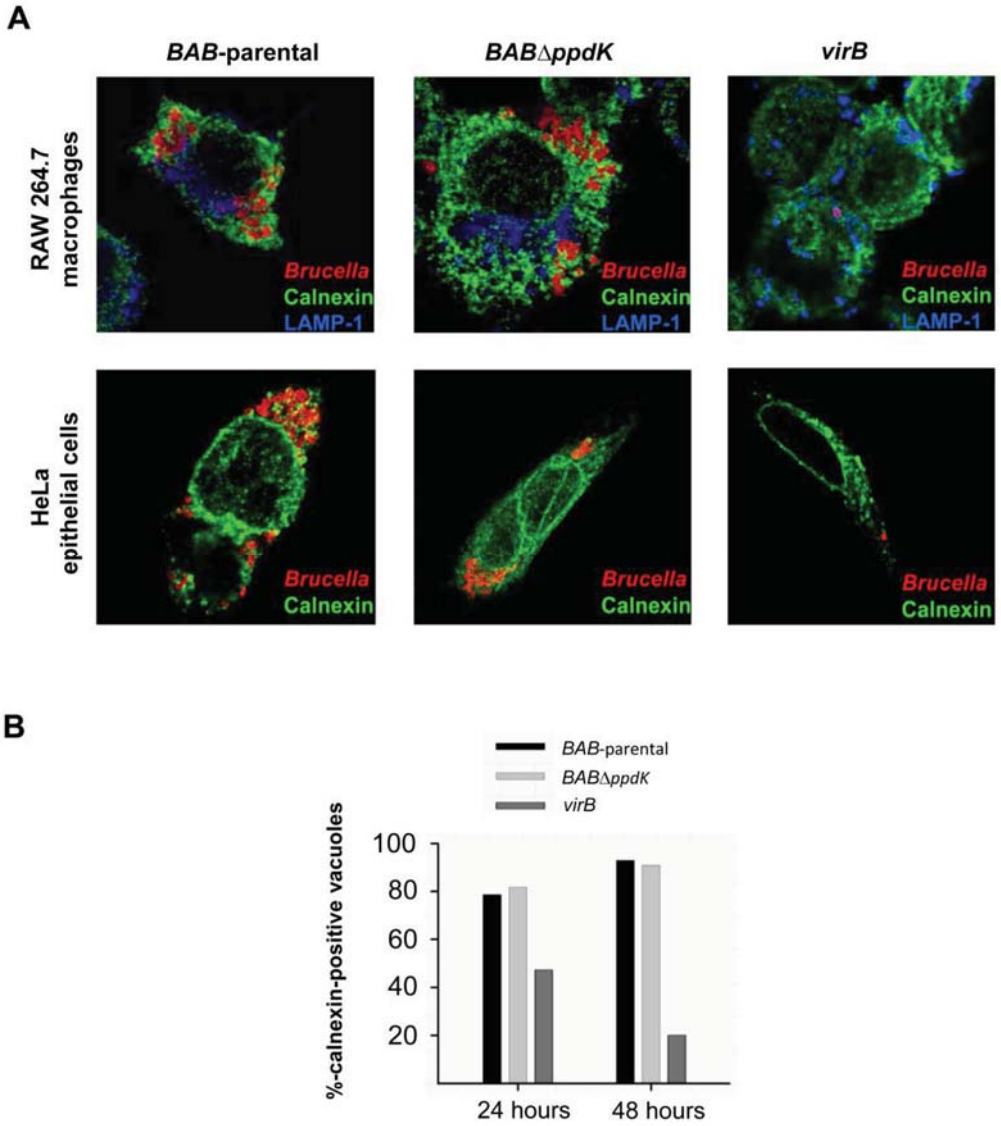

JB Accepts published online ahead of print